PARAMETRIC STUDY ON IMPROVEMENT OF G4(1S) STRONG POST GUARDRAIL SYSTEM

Jin Wu[1] and Ala Tabiei[2]

CENTER OF EXCELLENCE IN DYNA3D ANALYSIS
Department of Aerospace Eng. & Eng. Mechanics
University of Cincinnati, Cincinnati, OH 45221-0070
www.ase.uc.edu/~atabiei

ABSTRACT

The G4(1S) strong post guardrail system is the most common guardrail system in the USA. Full-scale crash testing indicated that the vehicle rolled onto its impact side after exiting the guardrail system. This collision behavior of the roadside structure increases the occupant risk and is considered unsatisfactory for safety. Improvement of the G4(1S) guardrail system becomes an important issue concerned by the FHWA. The subject of this investigation is to understand the system behavior through parametric study and present a feasible approach for structural improvement. This paper provides a roadmap for simulation of highway safety structures. Some of the noteworthy observations are presented and discussed. The approach of reducing the embedment depth of post is investigated through both FE component simulation and full system crash simulation. This approach is recommended and is anticipated to be favorable for minimizing the risk of rollover of vehicles impacting the G4(1S) guardrail system.

INTRODUCTION

Since the number of recent vehicles on the roads and the roadside obstacles continues to increase, roadway system analysis and design has become a primary goal of the Federal Highway Administration (FHWA). In the early 1960's, improvement of roadway safety structures was accomplished by proper engineering design through common sense to keep the vehicle and the occupant from turning over or being penetrated by roadside barriers. In the 1970's and 1980's, crash testing was developed to evaluate the collision behavior of roadside safety structures. Currently most of emphasis is still on conducting full-scale tests to gain insight into potential safety problems and develop new and improved roadside hardware. The design of roadside hardware such as guardrails, roadway signs and light poles under vehicle impact are performed experimentally through an iterative process of design, build, test, redesign and retest. This cycle continues until the product meets its design criteria.

Automobiles in use today cover a wider range of sizes and shapes than ever before, and there is a need to use different materials for certain parts of roadside hardware. As a result, many of the factors used in the design of highway safety structures should now be reconsidered. It is economically impossible to perform full-scale field testing on a wide range of parameters. Impact simulation utilizing nonlinear finite element (FE) analysis is thus rapidly becoming an effective tool in designing and evaluating these systems. FE crashworthiness simulations not

[1] Graduate Research Assistant
[2] Director

only can explain phenomenological behaviors of actual full-scale tests, but also can predict testing results a priori, and even evaluate untestable impact scenarios. FEA is well suited to parametric analysis and can provide enough information about stresses, strains, and accelerations of the roadside systems for structural modification and improvement. Although full-scale crash testing may never be eliminated, with the utility of FEA, it will no longer remain the primary tool for roadside safety research. The cost and time of designs will be substantially reduced. LS-DYNA (1997) is a powerful nonlinear, explicit, three-dimensional FE code. It has been used by the FHWA for computer simulation of vehicle impacts and crash events.

The G4(1S) strong post guardrail system is the most common guardrail system in the USA. The full-scale crash testing (Mak, 1995) indicated that the vehicle rolled onto its left side (impact side) after exiting the guardrail system. The vehicle thusly sustained severe damage. The impact performance of the G4(1S) guardrail system was considered unsatisfactory due to the rollover of the vehicle. The improvement of this system becomes an inevitable issue concerned by the FHWA. The objective of current investigation is to carry out parametric study on the G4(1S) guardrail system using LS-DYNA and provide a specific recommendation for structural improvement.

In previous papers (Tabiei, 2000), a roadmap for crashworthiness FE simulation of roadside safety structures was presented, and a finite element model was thus developed to accurately represent a full-scale crash test of the G4(1S) strong post guardrail as required by NCHRP Report 350 (Ross, 1993). This full system crash FE model was validated qualitatively and quantitatively. In the course of the validation, the FE model replicated the full-scale test within an allowable margin of error. This model enables us to identify the crash sensitive components of the G4(1S) guardrail safety structure under investigation. Identification of the sensitive parameters can be used as feed back in an optimization process to design new and improved guardrail system that will eliminate vehicle rollover. Once we are successful in validating one or more finite element models to represent full-scale crash tests, we have reached the point where the finite element simulation can be applied to new crash scenarios. Changing crash parameters, like critical angle of impact and vehicle speed, or the original design of the roadside safety structure will lead to an optimization process of the design of the roadside structure itself.

FULL-SCALE CRASH TEST

The full-scale crash test of the G4(1S) guardrail system was conducted by the Texas Transportation Institute (TTI) and the detailed information was provided by reference (Mak, 1995). A brief description is presented herein.

The test installation has a total length of 68.6 m (225 ft). The G4(1S) guardrail system consisted of 1.8 m (6 ft-0 in) long, W6×9 steel posts with 356 mm (14 in) long W6×9 steel blockouts, spaced 1.9 m (6 ft-3 in) on center and 3.8 m (12 ft-6 in) long 12-gange W-beam rail elements. The height of the guardrail to the center of the W-beam rail element was 550 mm (21.7 in). The W-beam rail elements were attached to the posts with 15.9 mm (5/8 in) diameter carriage bolts without any washers.

A 1988 Chevrolet 2500 pickup truck was used for the crash test. Test inertial mass or empty weight of the vehicle was 2,000 kg (4,409 lb) and its gross static mass or test weight was 2,075 kg (4,570 lb), including a restrained 50th percentile male anthropomorphic dummy placed in the driver’s position of the vehicle. The vehicle was directed into the installation using the cable reverse tow and guidance system, and was released to be freewheeling and unrestrained just prior to impact. The vehicle impacted the length-of-need section 0.61 m (2 ft) upstream of post 14, or 4.5 m (14.5 ft) upstream of the splice at post 16, traveling at a speed of 101.4 km/h (63.0 mi/h) at an angle of 26.1 degrees. The crash caused the deformation of the W-beam rail element between posts 14 through 18. There was evidence of sequential tire contact with posts 15, 16 and 17. The bolts were pulled out of the W-beam rail element at these three posts. When the vehicle exited the rail, it rolled 28 degrees counterclockwise and subsequently slid to rest on its left side (impact side). Table 1 summarizes the assessment of crash testing results from TTI. According to guidelines set forth in NCHRP Report 350, the impact performance of the G4(1S) guardrail system was considered unsatisfactory due to the rollover of the vehicle onto its left side which failed NCHRP 350 Occupant Risk Evaluation Criterion *F* as described in Table 1.

Table 1. Assessment of crash testing results with G4(1S) guardrail system (Mak, 1995)

NCHRP 350 Evaluation Criteria	**Assessment**
Structural Adequacy A. Test article should contain and redirect the vehicle; the vehicle should not penetrate, underride, or override the installation although controlled lateral deflection of the test article is accepted.	Pass
Occupant Risk D. Detached elements, fragments or other debris from the test article should not penetrate or show potential for penetrating the occupant compartment, or present an undue hazard to other traffic, pedestrians, or personnel in a work zone. Deformations of, or intrusions into, the occupant compartment that could cause serious injuries should not be permitted.	Pass
F. The vehicle should remain upright during and after collision although moderate roll, pitching and yawing are acceptable.	**Fail**
Vehicle Trajectory K. After collision it is preferable that the vehicle's trajectory not intrude into adjacent traffic lanes.	Pass
L. The occupant impact velocity in the longitudinal direction should not exceed 12 m/s and the occupant ridedown acceleration in the longitudinal direction should not exceed 20 G's.	Pass
M. The exit angle from the test article preferably should be less than 60 percent of test impact angle, measured at time of vehicle loss of contact with test device.	Pass

VALIDATED CRASH FE SIMULATION

In order to understand the collision behavior of G4(1S) strong post guardrail system, a full crash FE model, as presented in the previous paper (Tabiei, 2000b), was developed for an accurate simulation of a truck impacting the guardrail system as in the test. Both qualitative and quantitative validation indicated the presented FE model reasonably captured the basic sequence of events and could be used to improve the crashworthiness behavior of the G4(1S) guardrail system.

Three major issues are important when modeling the G4(1S) strong post guardrail for impact simulation. These issues are listed as follows:

1. Rail to blockout bolt connection.
2. Soil-post dynamic interaction.
3. Effect of ends of guardrail.

The modeling is described here in brief. Please see previous papers (Tabiei, 2000) for details.

Finite Element Model

The FE model of the G4(1S) strong post guardrail system is developed using the preprocessors HyperMesh (1995) and FEMB (1996). The FE model of the C-2500 pickup truck is provided by the National Crash Analysis Center (NCAC), and is imported into the guardrail model to generate a full system crash FE model (approximately 30,000 elements). Figure 1 shows the full FE model of the system. This full model is used to simulate the crashworthiness behavior of the guardrail system for evaluation of NCHRP Report 350 for the 2000-kg pickup truck recommendations.

Simulation of Bolt Connection

The W-beam is connected to the blockout with one bolt through a slotted hole. In the experimental testing of the guardrail system it is observed that some bolt connections are subjected to very high forces that cause the bolts to shear through the W-beam and result in the loss of bolt connection. This behavior is very important for accurate simulation of the impact event and drastically influences the redirection of the vehicle. In current FE crash model the bolt connection are simulated by nonlinear springs. The spring load curve for force-displacement is obtained through component simulation of bolt pull-out. As shown in Figure 2, the bolt is given a prescribed transverse displacement to travel through the W-beam. The nonlinear spring curve is accordingly defined with the contact force between the bolt and W-beam vs. the bolt displacement. The force value in the spring curve goes to zero once the bolt is completely pulled out through the W-beam. Therefore, the post and W-beam can continue to separate without any further force transfer, which is what happens in actual bolt failure. Since the bolt may be located in an arbitrary position relative to the hole in an actual guardrail system, two extreme cases (see Figure 3) are simulated and considered in the full crash model simulation to determine their effect on the total collision behavior.

Simulation of Soil-Post Interaction

The simulation of the soil-post interaction, which obviously plays a vital role in the response of the guardrail during an impact event, is a complex and important issue. Since it is computationally expensive to include the soil FE model in the impact simulation, an alternative method involving the use of nonlinear springs is utilized in simulation of the soil's response during loading. As shown in Figure 4, three dominant reaction components are considered in the modeling of soil-post interaction as follows:

- Soil-post force interaction in the direction perpendicular to the post web(in X-direction);
- Soil-post force interaction along the post web (in Y-direction);
- Soil-post torsional moment interaction about the axis of the post (about Z-direction).

The top left corner of Figure 5 shows a top view of a post with normal nonlinear axial springs K_1 and K_2 and nonlinear torsional springs K_3. These springs are attached to a master node and in turn the master node is attached to all nodes of the cross-section through rigid bodies. Consequently, forces in the springs are transferred properly to the entire beam cross-section.

The load curves of these springs are obtained through component simulation. Figure 5 depicts the FE model (7864 nodes and 7032 elements) developed for this purpose. It is a full-scale post imbedded in soil. For convenience the detailed analytical methodology is described in this paper later. Also see previous papers (Tabiei, 2000) for details.

Simulation of End of Guardrail

The test setup for the G4(1S) system consisted of a 68.6 m guardrail section. The finite element model of the entire system is impractical and computationally inefficient and therefore, a simulated end effect must be included in the proposed FE model. Accurate simulation of the G4(1S) system is very much dependent on the accurate representation of the unmodeled portions. Since the W-beam redirects impacting vehicles primarily through beam tension, elastic springs are attached to the ends of the modeled W-beam to simulate its continuation in both directions. Initially, the stiffness of the spring is derived from the following relationship:

$$K = \frac{EA}{L}$$

where E is the steel modulus of elasticity, A is the W-beam cross-section, and L is length of the unmodeled portion of the beam. This modeling ignores the effects of terminal movement and the effects of rail-splice “slip” during the impact. This approximation is investigated by developing a detailed finite element model of the unmodeled portion of the guardrail (L = 25.7 m). The detailed model accounts for the effects of bolt connection and soil-post interaction. It is assumed that the effect of bolt sliding in the blockout-rail connections is insignificant. The SECFORC option is invoked in LS-DYNA to determine the cross-section forces. Very good correlation is observed between the above simple linear spring relation and simulated results from the detailed model with a fixed end terminal. The simple linear spring relation overestimates the stiffness of the roadside safety structure, and is therefore not well suited to simulate the full-scale crash test of the G4(1S) guardrail system.

Full-scale crash testing of G4(1S) guardrail system indicated that the installation received moderate damage at the end of the terminal. The large lateral deflection of W-beam caused the movement of the end terminal through beam tension. To accurately represent this realistic behavior, the effect of terminal movement has to be considered in the full system FE model. For this purpose, in the above detailed model the fixed constraints are removed and the end terminal is thus allowed motion. The model includes the W-beam and the posts as well as soil-post interaction. The end terminal of the guardrail is assumed to be connected to a post. This post is connected to several distributed springs that represent the stiffness of the soil. A prescribed displacement is acted at the front end of W-beam, and the SECFORC option is invoked to determine the cross-section forces. The evaluated stiffness of the elastic spring is shown in Figure 6, which is about 20 percent of the simple linear spring stiffness. Current spring stiffness considers the terminal movement and yields better results in full system crash simulations.

Validation of Full System Crash Simulation

The full system crash simulation was performed on the computing platform Cray T94 at the Ohio Supercomputer Center. The sequential photographs were compared between the test and simulation for qualitative validation. The comparative figures indicated that the finite element simulation reasonably captured the basic sequence of impact events. Bolt pull-out and wheel snagging phenomena were also observed in the finite element simulation. The quantitative validation was accomplished by comparing the acceleration at the center-of-gravity of vehicle obtained from the full-scale test and simulation (see Figure 7). The following three NARD quantified validation measures were used in the study:

- Relative Absolute Differences of Moments;
- Root Mean Square (RMS) Log Measure of Difference;
- Energy Measure of Correlation.

All Relative Absolute Differences of Moments are less than 0.20, which is considered an acceptable correlation value. See the previous paper (Tabiei, 2000b) for details.

The validated full system crash FE model replicated the basic phenomenological behavior of the actual full-scale test, and therefore enables us to identify the crash sensitive components of the G4(1S) guardrail safety structure and finally figure out a feasible approach for the system improvement which is much concerned by the FHWA. In this paper, the investigation is aimed at understanding the crashworthiness effects of variation of some G4(1S) guardrail systematic parameters. Identification of critical parameters that alter the crash behavior and the load path is carried out in this investigation. This is useful for design improvement of the G4(1S) structure for elimination of vehicle rollover. Several attempts have been performed for improvement of the G4(1S) guardrail system. They are presented in separate sections below.

ATTEMPTS FOR ELIMINATION OF WHEEL SNAGGING

Wheel snagging is one of the most important factors directly influencing the truck rollover. Initial study was aimed at the elimination of wheel snagging. This was conducted by some minor modifications of the components of G4(1S) guardrail system. These modifications are listed as follows:

1. Increasing post spacing.
2. Reducing the height of the guardrail system.
3. Replacing steel blockouts with wooden blockouts.
4. Using wooden blockouts and reducing post spacing.
5. Using large-sized wooden blockouts.

All of the modifications were based on the validated full crash FE model. Several dozen simulations were carried out. The duration of each FE simulation was 180 milliseconds which was considered enough for the observation of the system behavior with respect to wheel snagging. The simulated results are described in the following sections.

Increasing Post Spacing

In this modification the post spacing was extended for the guardrail system. The expansion of the post spacing could increase the time for the vehicle to travel from one post to another. It was expected that the left-front wheel of the vehicle might yaw enough to avoid contacting the next post as the vehicle traveled.

In the modified guardrail system, the steel posts were spaced 2.85 m on center (150 percent of the original post spacing) instead of 1.9 m. There was no change in any other system parameter. The crash simulation indicated that the modified guardrail system had less lateral stiffness. The simulated deflection of W-beam became larger. The reduction in the lateral stiffness could buffer the vehicle-guardrail impact, however, it was not favorable with respect to increasing the swerve of the truck. A large twist occurred on post 14 (see Figure 8). The left-front tire of vehicle didn’t yaw enough and snagged on post 15. The left tire was uplifted. At post

15 the bolt pull-out phenomenon was observed. The loss of rail-blockout connection provoked the large deformation of the W-beam. The rail warped to a lower elevation and the left-front wheel traveled over the rail at that location as shown in Figure 8.

Reducing the Height of the Guardrail System

The elevation of the guardrail has an important effect on the contact area between the W-beam and left-front wheel. If the contact location is closer to the rotation center of the wheel, the wheel may be redirected easier. In general it is possible to eliminate the interaction between the wheel and posts. For this purpose, a FE simulation was performed here to study the effect of this parameter.

In the modified FE model the height of the guardrail to the center of the W-beam rail was changed to 470 mm from the original elevation of 550 mm. The embedment depth of the posts was assumed to remain the same. When the impact started, initially a large torsional deformation was observed on post 14. As the vehicle traveled to post 15, wheel snagging occurred and the left-front wheel was uplifted. The bumper of vehicle consequently pushed the W-beam rail to a lower elevation and redirected the left-front tire to surmount the W-beam rail (see Figure 9). Although the behavior of the vehicle was the same as in the previous simulation (see Figure 8), the provocation was different. In the previous case, the overpass of the truck came from the large deformation of the W-beam. However, in current simulation the bumper exhibited a redirectional role, which was caused by the reduction of the guardrail height.

Replacing Steel Blockouts with Wooden Blockouts

Comparing the results of the above two simulations (see Figures 8 and 9), one can observe the large torsional deformation of the upper portion on post 14. In order to improve the crashworthiness behavior of the guardrail system, it is expected to increase the deflection of posts along the direction perpendicular to the W-beam. The occurrence of large torsion of posts has a disadvantageous effect on this expectation. Since the I-beam steel blockouts are used in the G4(1S) guardrail system, the level of the interaction between the rail and posts is very much dependent on the rigidity of the blockouts. The web of the blockouts plays a significant role in the force transfer along itself. Buckling of the web could cause collapse of the load transfer and result in large torsional deformation of the post. Current modification was designed to investigate the effect of buckling of the blockouts on the vehicle kinematics.

Since wood material is often used in roadside safety structures, the modified guardrail system was installed with wooden blockouts instead of steel blockouts. The simulation indicated that no buckling phenomenon could be detected on wooden blockouts. Compared with the above two simulations, the twist of post 14 has been efficiently reduced. It indicates that the blockouts could transfer more interaction forces from the rail to the posts and the posts are allowed more movement along their web direction. It is favorable for improvement of the guardrail system. However, current modification can not eliminate the wheel snagging. It was still observed in the simulation (see Figure 10).

Using Wooden Blockouts and Reducing Post Spacing

Since the use of wood blockouts is advantageous for guardrail improvement, this modification is also considered in the FE model here. Appropriate increase in the lateral stiffness of guardrail could cause an earlier swerve of the truck and more movement of the posts along their web direction. It might reduce the possibility of wheel snagging on the posts. In this modification, the increase of the lateral stiffness was achieved by reducing the post spacing.

In the FE model with wooden blockouts, the steel posts were spaced 1.425 m on the center (75 percent of the original post spacing) instead of 1.9 m. The simulation displayed less lateral deflection of the modified guardrail. The left-front tire of vehicle first snagged on post 15 and turned toward the W-beam. It caused excessive decelerations of the vehicle. As the tire traveled to engage post 16, severe deformation was observed in the tire (see Figure 11). In an actual impact event this will cause tire deflation and possibly separation of wheel assembly from the vehicle. This modification is therefore considered to be a failure with respect to safety improvement.

Using Large-Sized Wooden Blockouts

In this modification a large-sized blockout was considered to increase the lateral space between the post and W-beam rail. This modification was expected to eliminate tire-post contact.

As shown in Figure 12, the guardrail system was installed large-sized wooden blockouts whose size was doubled along the post web. The post spacing remained the same as the original value of 1.9 m. As depicted in the simulation, although the posts were set backward to avoid contacting the left-front tire of vehicle, the wheel still snagged on posts 15 and 16. The increase of the lateral space was insignificant for the traveling vehicle. The torsion of post 14 was satisfactory. However, very large torsional deformation (more than 180 degrees) occurred on post 16 (see Figure 12). This behavior illustrated that the increase in the size of wooden blockouts could allow more torsional moments to be transferred to the posts and cause unfavorable deformation on them. It has a disadvantageous effect on the collision behavior of guardrail system.

The above attempts indicate that for a vehicle traveling with a high velocity (around 65 mi/hr) it is difficult to eliminate wheel snagging only through minor modifications of the guardrail system. There are many parameters influencing the rollover of vehicle upon impact in the G4(1S) guardrail system. It is a very complicated issue to quantitatively investigate each individual effect of these parameters. For improvement of this system it is necessary to figure out an economic and feasible approach to overwhelm the problem of vehicle rollover. This approach should improve the energy-absorption capacity of the W-beam rail to buffer the impact and contain the errant vehicle. As mentioned previously, the use of wooden blockouts could increase the deflection of posts along the direction perpendicular to the W-beam. It is advantageous for the improvement of guardrail system.

EFFECT OF EMBEDMENT DEPTH OF POST

In current study, one of the important factors, *embedment depth of post*, has been investigated. It is found that appropriate reduction of the embedment depth could weaken the soil-post interaction and allow more displacement of post in the web direction. The lateral stiffness of guardrail system becomes less. And more dissipated energy could be absorbed by the W-beam rail during the impact. Compared with the use of wooden blockouts, this approach is more simple and acceptable. The detailed simulation results are presented in the following sections.

Component Simulation of Soil-Post Interaction

As mentioned previously, three reaction components are assumed to dominate the soil-post interaction. They are the soil-post force interaction perpendicular to and along the post web and the torsional moment interaction about the axis of the post. In the full crash FE model, nonlinear axial and torsional springs are utilized in simulation of these three soil-post interaction components as depicted in Figure 4. The load curves of nonlinear springs are obtained through individual component simulations (see Figure 5). For instance, to define the nonlinear axial springs perpendicular to or along the post web (along the x or y direction in Figures 4 and 5), a lateral prescribed constant velocity is applied at the upper portion of the post model (550 mm above grade) in x or y direction. The SECFORC option is invoked to obtain the cross-section x- or y-forces of post at several locations (at A, B, C, … etc. in Figure 5) in the soil-post FE model. The cross-section cutting planes cleanly pass through the middle of the elements of the post. In this way, the cross-section cutting planes are such made that one can always find a node of the post axis in the middle of any two adjacent cross sections. The nodal x- or y-displacement data of the post axis can be obtained from the NODOUT file. Let's consider the portion of post between any two adjacent cross sections as a unit. Figure 13 illustrates a schematic diagram for evaluating the load values used to define axial springs. In the small embedded portion of the post with the mass M, since the applied velocity remains constant, the acceleration of the mass M is ignored. The interaction force from the soil, F_{soil}, can be easily calculated through equilibrium. In the full crash FE model, a nonlinear axial spring is added to the location of the node in the middle of these two cross sections. The interaction force between the soil and this portion of the post is taken as the difference between the cross-section forces ($F_{A'}$ and $F_{B'}$). The load curve of the nonlinear spring is thus defined with the interaction force vs. nodal displacement. In a similar fashion, the load curves of nonlinear torsional springs can also be obtained.

In this study, FE component simulations (see Figure 5) have been performed on two soil-post interaction models with different embedment depth of post. One of cases considered, the original embedment depth remains the same (1120 mm) as in the actual G4(1S) guardrail system. The other case considered the embedment depth has been changed to 840 mm (75 percent of the original value). The material properties of the soil (see Tabiei 2000b), as proposed in reference (Schauer, 1997), are used in the simulations. Figures 14 through 19 show the simulated results for nodal displacements (or rotations) of the post axis and cross-section forces (or moments) on the post. These data are filtered at 30 Hz. The nodal data curves are organized from grade to the lower portion of the post in an alphabetical order. The distance between two adjacent nodes is 70 mm. In the same fashion, the cross-section forces are shown from 35 mm above grade to the lower depth. The interval of two adjacent cross sections is also 70 mm. In Figures 14 through 16, we can see that nodal deformation of the post axis descends to negative values as the depth of nodal location increases. This indicates that there exists a "static" point of inflexion above which the deformation is positive. Corresponding to three dominant soil-post interaction components, there are three individual "static" points of inflexion. The location of the points can be evaluated by analyzing the deformation of the post axis (see Figures 14 through 16) or discovering the critical point for the sign change of the difference between two adjacent cross-section forces or moments (see Figures 17 through 19). It is observed that the "static" point of inflexion with respect to the reaction component along the post web is located at the deepest level. In the full crash FE model, the nonlinear springs are placed above this point to simulate the soil-post interaction. A proper pinned constraint is imposed on this point of inflexion. In this manner there would not be a need to model the post-soil interaction below this point.

For the posts with the same cross sections, the soil-post interaction is dependent on the embedment depth. Table 2 describes a comparison of the simulated results between the embedment depth of 1120 mm and 840 mm. It indicates that reducing the embedment depth mainly influences the soil-post interaction component along the post web. After reduction of the embedment depth of post, the central displacement on the post cross section at grade has an increase of 14.7 percent in this direction. The corresponding point of inflexion has ascended and shifted to 560 mm below grade. In the other directions, less change is observed in deformation. The individual location of point of inflexion tends to move down.

Table 2. Soil-post simulation results for different embedment depth of post

Time = 0.1 s		**Embedment Depth**		**Relative Difference Ratio**
		1120 mm	**840 mm**	
Central Displacement or Rotation on Post Cross Section at Grade	Vertical to the Post Web (mm)	98.2	95.3	-3.0%
	Along the Post Web (mm)	149.6	171.6	14.7%
	About the Post Axis (radian)	0.38	0.40	5.3%
Location of Point of Inflexion (mm, below grade)	Deflection vertical to the Post Web	350	490	40%
	Deflection along the Post Web	700	560	-20%
	Rotation about the Post Axis	420	490	16.7%

Comparison of Crash Simulations between Original and Modified Guardrail System

The component simulations of soil-post interaction indicate that appropriate reduction of the embedment depth of post could allow more movement of the post in the web direction. It might make the actual guardrail system have less lateral stiffness and absorb more energy in impact events. To verify this point, the G4(1S) guardrail system was modified to include the posts with the embedment depth of 840 mm instead of 1120 mm. Another vehicle-guardrail FE model is thus built for current investigation. Compared with the original validated FE model, this new model only has minor modifications obtained from the new simulations of soil-post interaction. Fifteen normal axial springs (seven vertical to the post web and eight along the web) and seven torsional springs are employed for each post in the modified FE model. A pinned constraint is imposed on each post at 560 mm below grade rather than 700 mm in the original model. Figures 20 and 21 describe the nonlinear axial springs in the original and modified FE models for simulation of soil-post interaction along the post web. The crash simulation of the modified FE model is performed on the same computing platform (Cray T94). The simulations of these two FE models are compared qualitatively and quantitatively as follows.

- ***Qualitative Comparison***

Qualitative comparison is achieved by comparing the sequential views (overhead and frontal views) obtained from both simulations. Figures 22 and 23 depict the simulated behavior for both guardrail systems. In these figures the modified guardrail system with less embedment depth of post and the pickup truck are represented in a mesh mode. While the vehicle of the original FE model is represented in a shaded mode. No original guardrail structure is shown in the figures. In this manner the difference between the two runs can be clearly detected.

Bolt pull-out and wheel snagging phenomena are observed in both simulations. During the initial period of impact no distinct difference can be observed between the simulation results. The rotation of the vehicle ceases to be the same after 0.20 second. Then the divergence gradually becomes noticeable. The comparative figures indicate that the vehicle impacting the modified guardrail system has less yaw and roll rotations during the impact event. In this type of angle impact collision the redirection of the vehicle mainly depends on the stiffness of the guardrail. The reduction of rotation of the vehicle implies that the vehicle-guardrail contact forces are less and the impact has been more contained. It indicates that appropriate reduction of the embedment depth of post could decrease the lateral stiffness of the guardrail and improve the energy-absorption capacity for the W-beam.

- ***Quantitative Comparison***

In order to gain further understanding of the effect of the embedment depth of post on the crashworthiness behavior of the guardrail system the simulations are also compared quantitatively. Figure 24 depicts the time history of the vehicle angular displacements in different orientations. The axes are fixed in the bed of vehicle to determine these orientations (yaw, roll and pitch). It can be observed that the divergence of the yaw rotation in these two simulations occurs at about 0.20 second. The roll rotation ceases to be the same at about the same time. After about 0.20 second a distinct difference is detected between these two simulations. Comparison of kinematics indicates that the rotations of vehicle, both in yaw and roll, have been effectively reduced by modification of the embedment depth of post. However, the simulated pitch rotation in the modified FE model is larger than the original one.

The lateral deflection of the W-beam is compared in Figure 25. The time-history data describe the lateral deflection of the W-beam at the location of posts 15, 16 and 17. These posts have the greatest interaction with the impacting vehicle. Compared with the simulation of the original FE model, the modified guardrail system exhibits less lateral stiffness. As the vehicle travels, the modified FE model displays a larger lateral deflection of W-beam at the location of these posts sequentially. The distinct difference of the lateral deflection occurs at about 0.13 second at post 15, 0.20 second at post 16, and 0.30 second at post 17. The rail deflection at post 17 has been substantially increased by reducing the embedment depth of post.

In order to minimize the risk of rollover, roadside safety structures are always expected to have greater capacity to absorb more energy in an impact event. In this study, the energy (kinetic energy and internal energy) absorbed by the W-beam is compared between the two simulations and depicted in Figure 26. The comparison indicates that the energy absorption has been increased significantly after the modification. The initial discrepancy occurs at 0.16 second. After the vehicle exits the guardrail system, the absorbed energy has been increased up to 182% which evidently verifies the efficiency of the present approach. The modification through reducing the embedment depth of post will improve the G4(1S) guardrail system to overwhelm the problem of vehicle rollover. Table 3 provides a summarized comparison between the original and modified FE model simulations. The time of 0.53 second is considered because the vehicle in the original FE model loses contact with the guardrail at about 0.53 second just as in the actual crash test.

Table 3. Comparison of simulated results between two FE crash models

Time = 0.53 second			Original FE Model	Modified FE Model
W-Beam Rail Element	Lateral Deflection at Post#17, m		0.165	0.277
	Absorbed Total Material Energy (Kinetic Energy + Internal Energy), N×m		3.59×10^5	6.54×10^5
Vehicle	Angular Displacement, degrees	Yaw	45.5	33.2
		Roll	-20.5	-1.06
		Pitch	-8.32	-10.1
	Velocity at Center-of-Gravity, km/h		54.7	43.6

DISCUSSION AND CONCLUSIONS

Full-scale crash testing of the G4(1S) strong post guardrail system indicated that this roadside structure caused the rollover of the vehicle and was considered unsatisfactory according to guidelines set forth in NCHRP Report 350. The improvement of this guardrail system becomes one of the important issues concerned by the FHWA for occupant safety. Current investigation provides a roadmap for modeling and simulating the G4(1S) guardrail system. Based on a validated full system crash FE model, parametric study is presented in this paper for understanding the effects of component modifications of the G4(1S) guardrail system. This is useful for improvement of the G4(1S) system to eliminate vehicle rollover. Some of the noteworthy observations are summarized as follows:

- Wheel snagging is one of the most important factors directly influencing the vehicle rollover. For a vehicle with a high traveling velocity (around 65 mi/hr) it is difficult to eliminate wheel snagging with only minor modifications of the guardrail system.
- The use of wooden blockouts could eliminate the buckling of blockouts and allow the posts more movement along their web direction. It is advantageous for the improvement of the guardrail system.
- Component simulation has proved to be a powerful tool which can be used before full system crash model simulation. Soil-post interaction simulation shows that the embedment depth of W6×9 steel post mainly influences the reaction component along the post web which plays an important role in the lateral stiffness of roadside structures.
- Full system crash simulations indicate that appropriate reduction of the embedment depth of post could weaken the soil-post interaction and produce more displacement of post in the web direction. It will decrease the lateral stiffness of guardrail system and allow the W-beam

to absorb more energy in an impact event. The yaw and roll rotations of the vehicle are thus reduced efficiently in the modified guardrail system.

The approach of reducing the embedment depth of post has been submitted to the FHWA as a recommendation for improvement of the G4(1S) guardrail system. This modification is anticipated to be favorable for minimizing the risk of rollover of vehicles impacting the G4(1S) guardrail system. In current study this approach is investigated through numerical simulations. Its reliability still needs further verification by full-scale crash tests.

ACKNOWLEDGMENTS

The Center would like to thank the FHWA for supporting this project under a collaborative agreement. Many thanks should also be advanced to Mr. Martin Hargrave the contract monitor and Mr. Charlie McDevitt for their valuable advice. Computing support was provided by the Ohio Supercomputer Center. Their support is gratefully acknowledged.

REFERENCES

1. FEMB User’s Manual, Version 26.5, Engineering Technology Associates, Inc., Madison Heights, MI, 1996.
2. HyperMesh Manual, Version 2.0, Altair Engineering, Inc., Troy, MI, 1995.
3. LS-DYNA User’s Manual, Version 940, Livermore Software Technology Corporation, 1997.
4. Mak, K. K., Bligh, R. P., and Menges, W. L. (1995). Crash testing and evaluation of existing guardrail systems, Texas Transportation Institute, No. RF 471470.
5. Ross, H. E., Jr., Sicking, D. L., Zimmer, R. A. and Michie, J. D. (1993). NCHRP Report 350, Recommended procedures for the safety performance evaluation of highway features, Transportation Research Board, Washington, D.C.
6. Schauer, D., Tokarz, F., Kay, G., Lee, A., Logan, R., Coffie, E. and Ray, M. (1997). Preliminary vehicle impact simulation technology advancement (Pre-VISTA), Publication No. FHWA-RD-96-059, Federal Highway Administration.
7. Tabiei, Ala, and Wu, Jin (2000a). “Roadmap for crashworthiness finite element simulation of roadside safety structures.” *Finite Elements in Analysis and Design*, Vol. 34, pp. 145-157.
8. Tabiei, Ala, and Wu, Jin (2000b). “Validated crash simulation of the most common guardrail system in the USA.”, *International Journal of Crashworthiness*, Vol. 5, pp. 153-168.

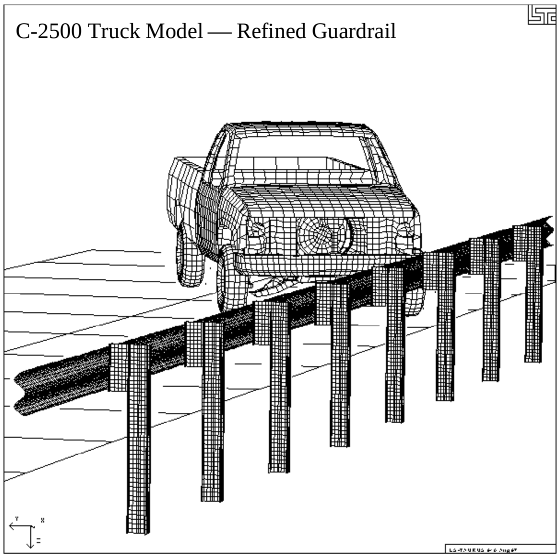

Figure 1. Vehicle and G4(1S) FE model

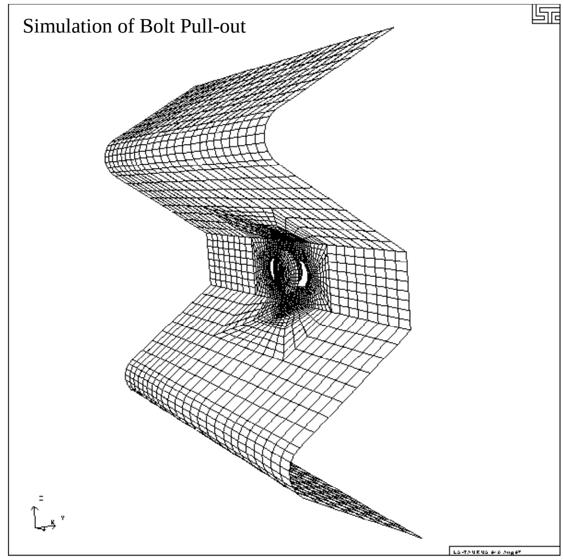

Figure 2. FE model for simulation of bolt pull-out

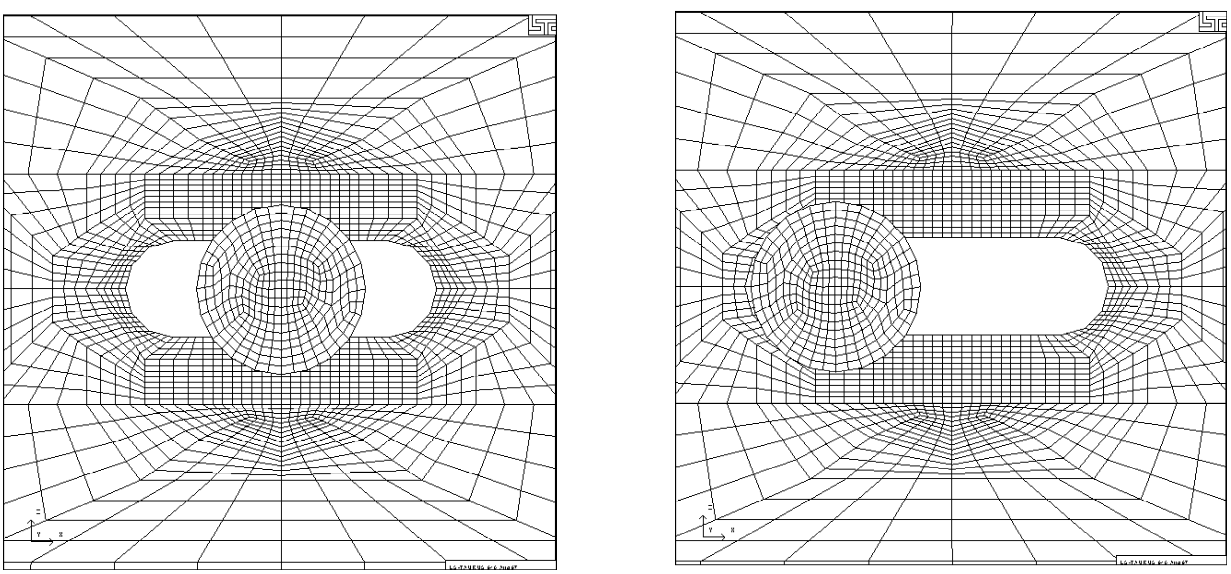

(a). bolt at the center of the hole

(b). bolt offset from the center of the hole

Figure 3. Bolt location in simulation of bolt pull-out

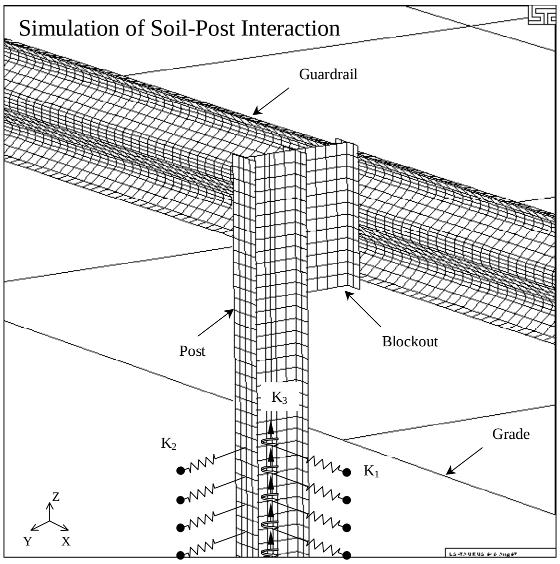

Figure 4. Simulation of soil-post interaction

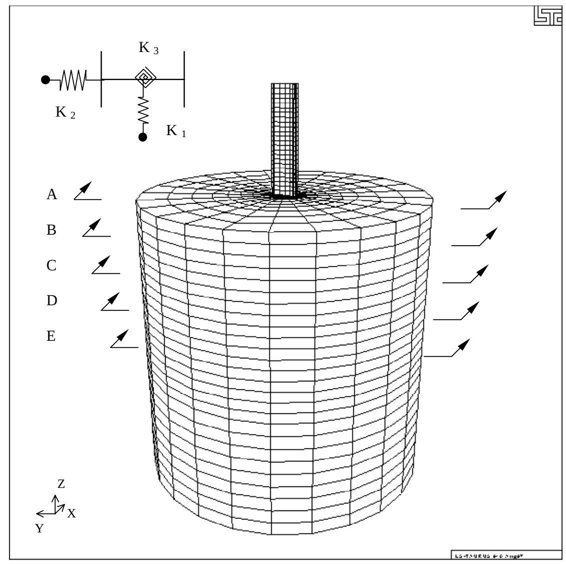

Figure 5. Component simulation of soil-post interaction

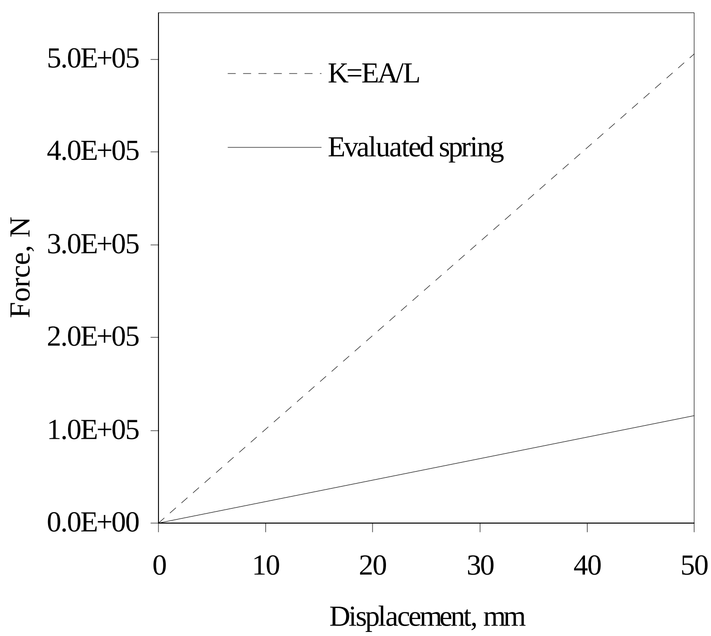

Figure 6. Elastic spring stiffness for simulating the end effect of guardrail

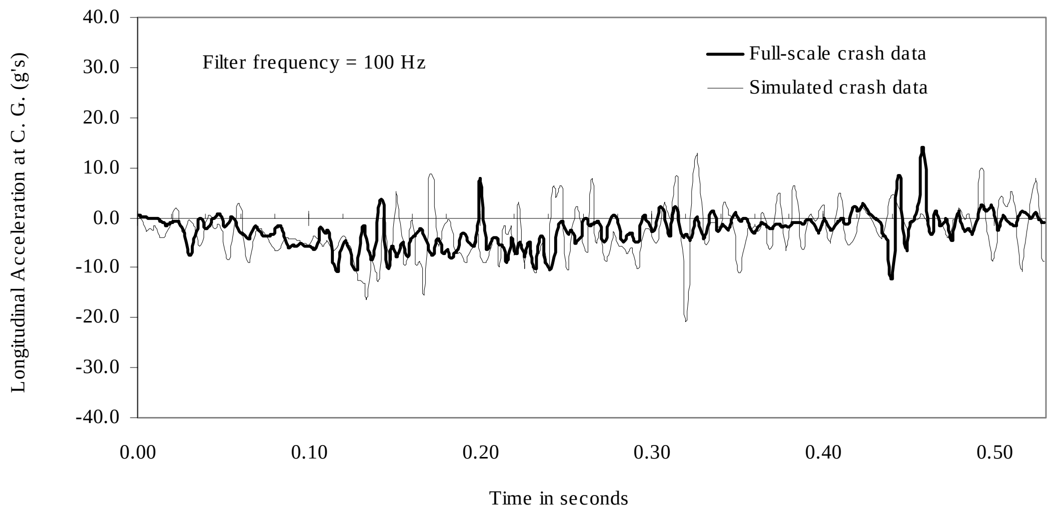

Figure 7. Longitudinal acceleration at center-of-gravity

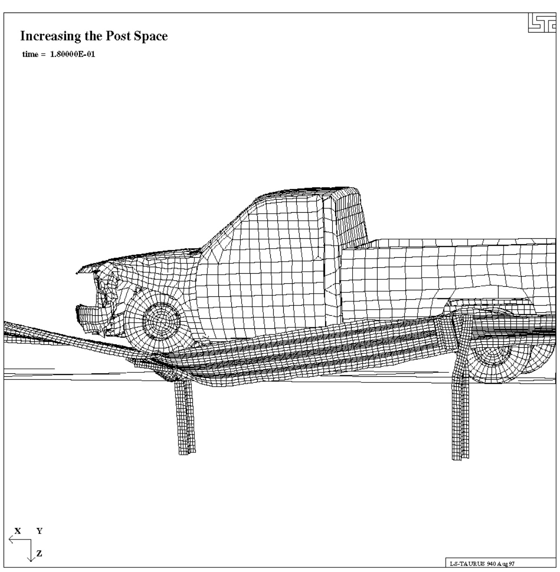

Figure 8. Increasing post spacing

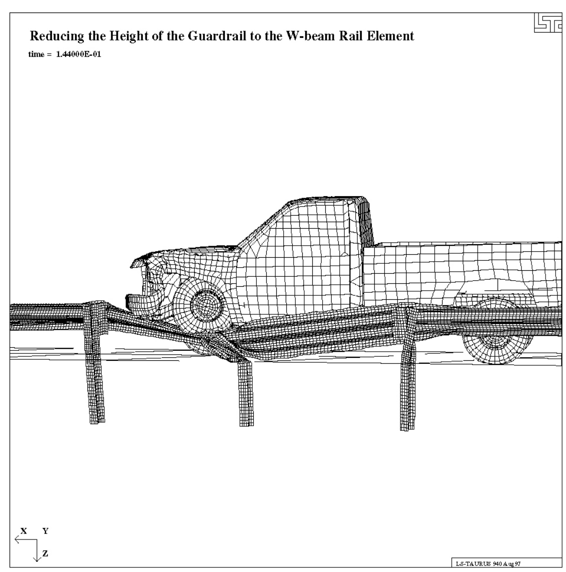

Figure 9. Reducing the height of the guardrail system

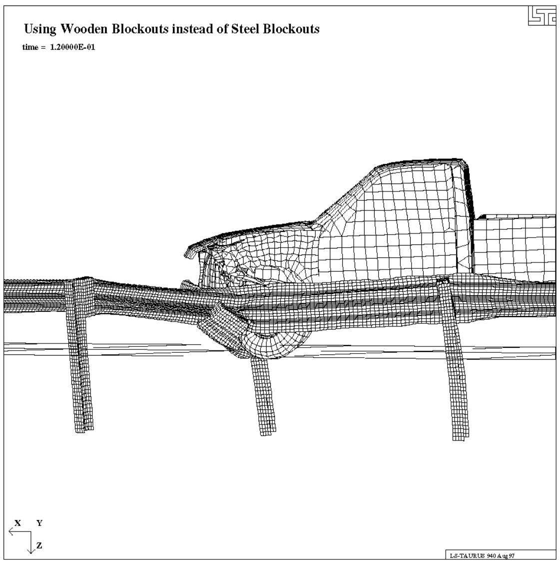

Figure 10. Use of wooden blockouts

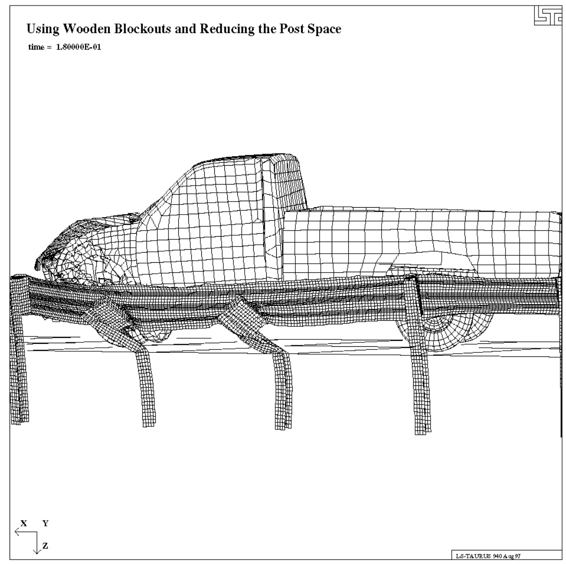

Figure 11. Wooden blockouts & reduced post spacing

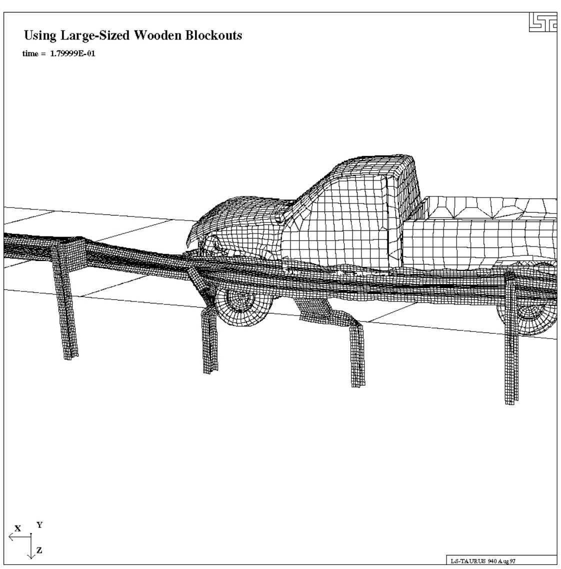

Figure 12. Using large-sized wooden blockouts

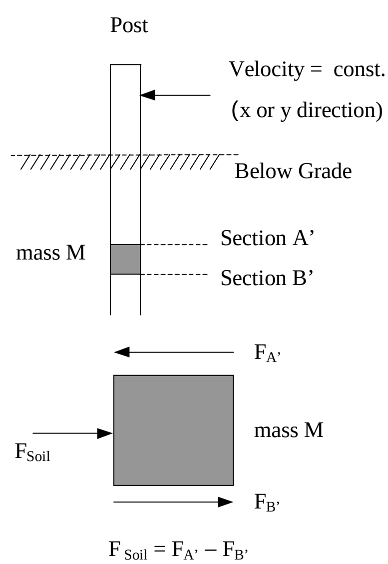

Figure 13. Calculation of soil-post interaction forces

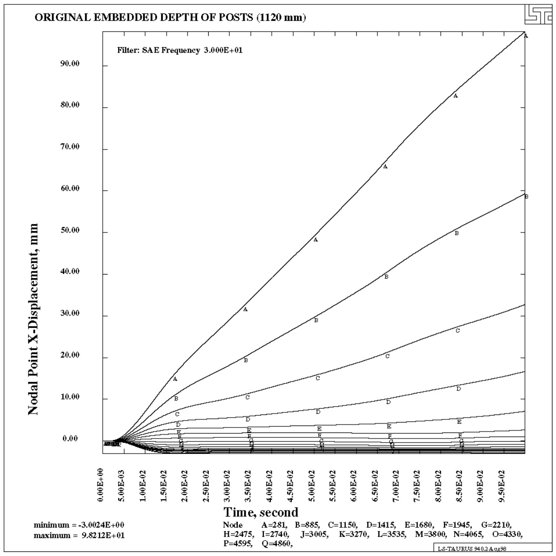

(a). Embedment depth of 1120 mm

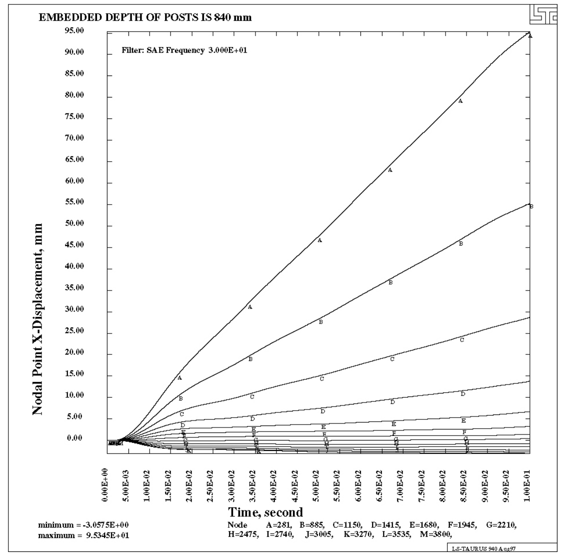

(b). Embedment depth of 840 mm

Figure 14. Nodal displacements on the post axis (perpendicular to the post web)

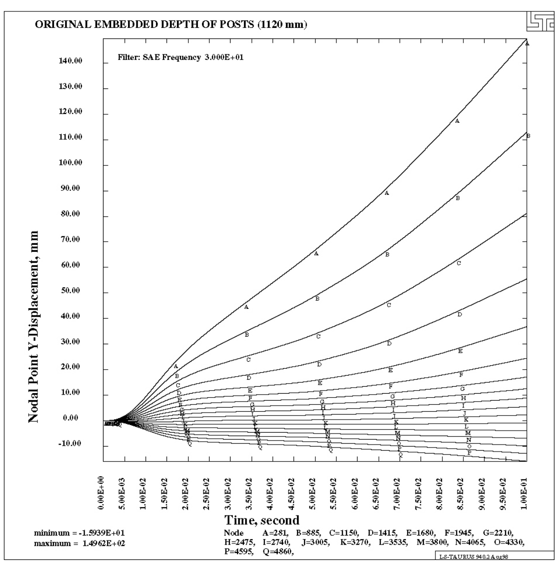

(a). Embedment depth of 1120 mm

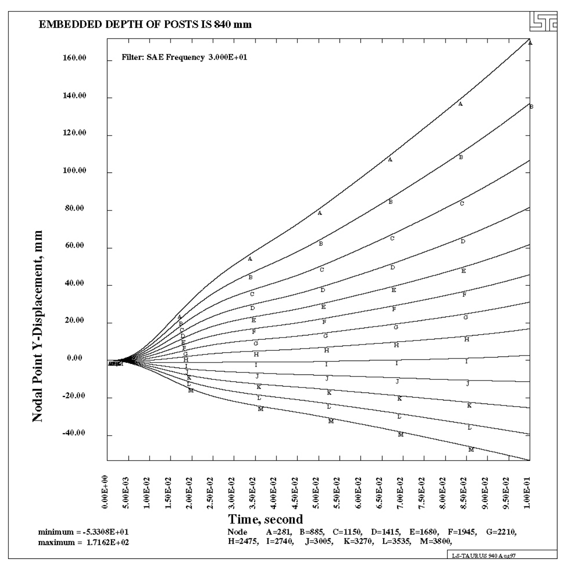

(b). Embedment depth of 840 mm

Figure 15. Nodal displacements on the post axis (along the post web)

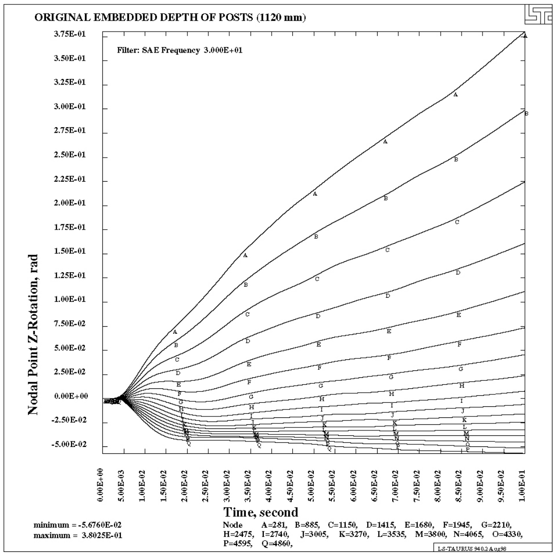

(a). Embedment depth of 1120 mm

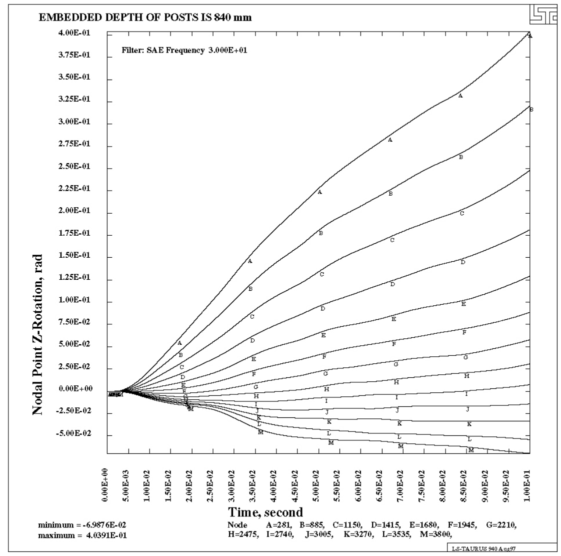

(b). Embedment depth of 840 mm

Figure 16. Nodal rotations on the post axis (about the post axis)

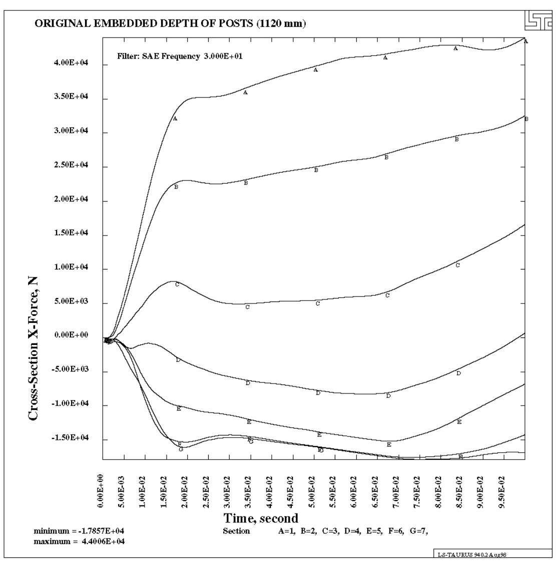

(a). Embedment depth of 1120 mm

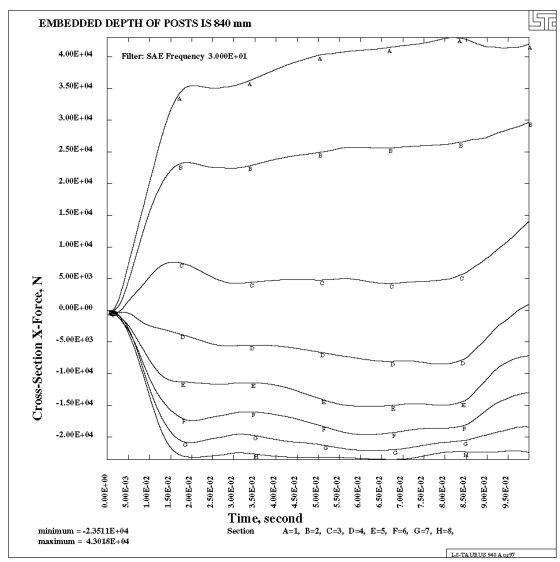

(b). Embedment depth of 840 mm

Figure 17. Cross-section forces perpendicular to the post web

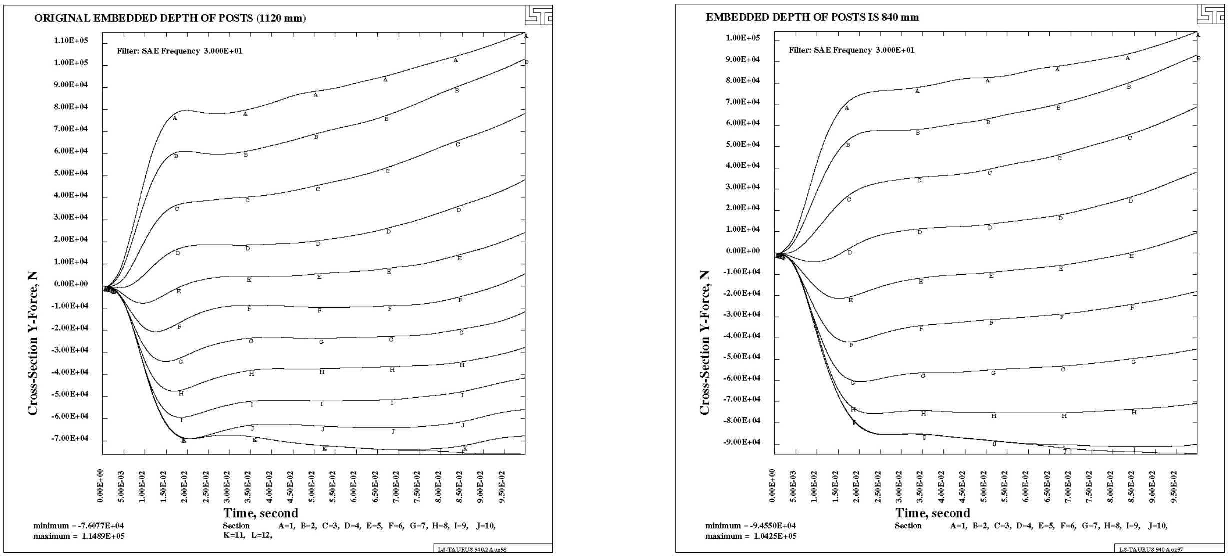

(a). Embedment depth of 1120 mm (b). Embedment depth of 840 mm

Figure 18. Cross-section forces along the post web

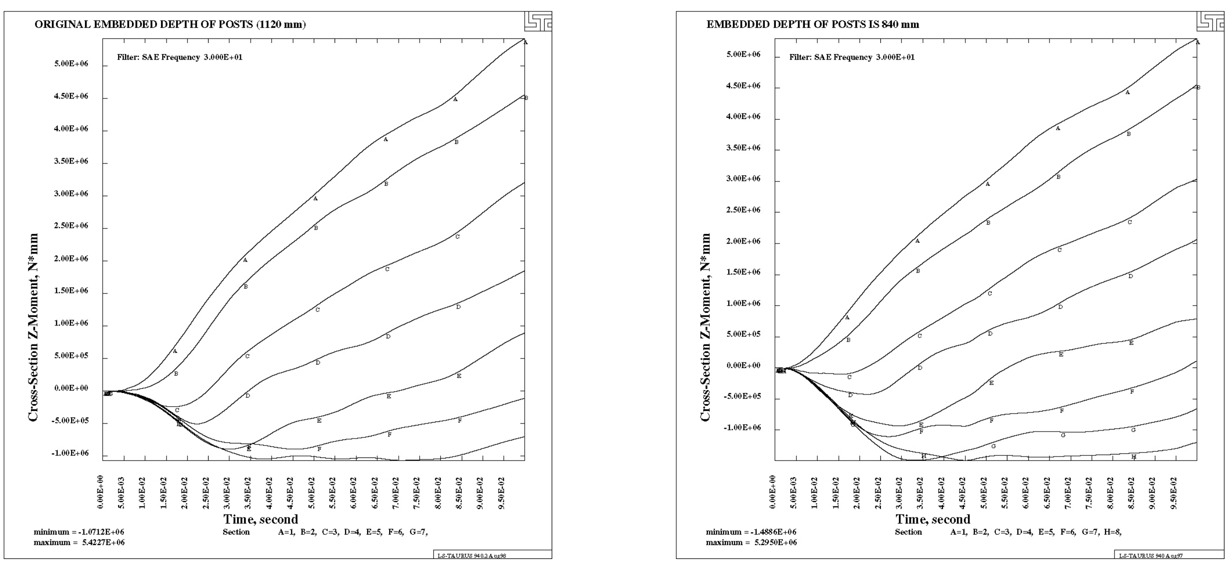

(a). Embedment depth of 1120 mm (b). Embedment depth of 840 mm

Figure 19. Cross-section moments about the post axis

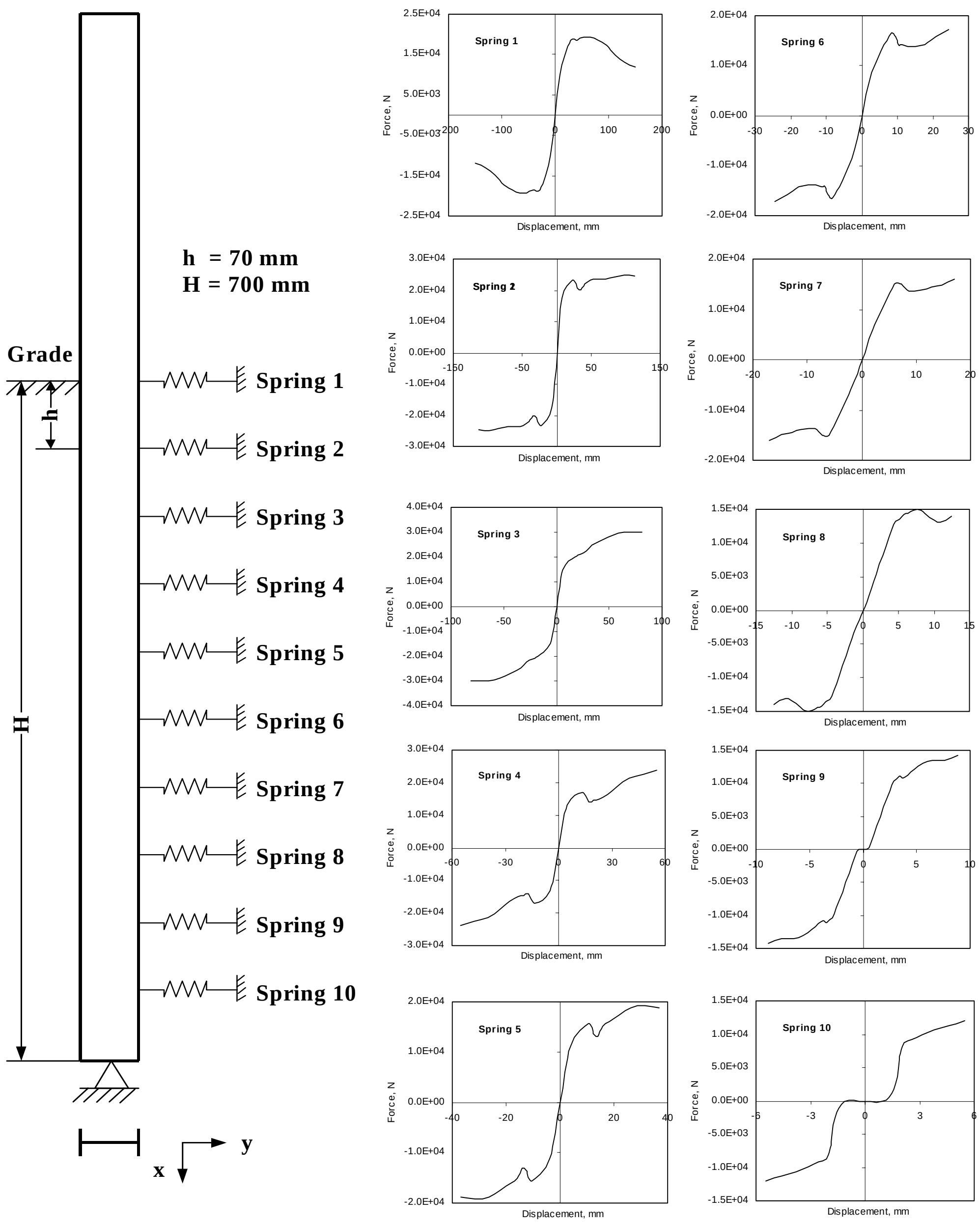

Figure 20. Nonlinear axial springs in the original FE model (along the post web)

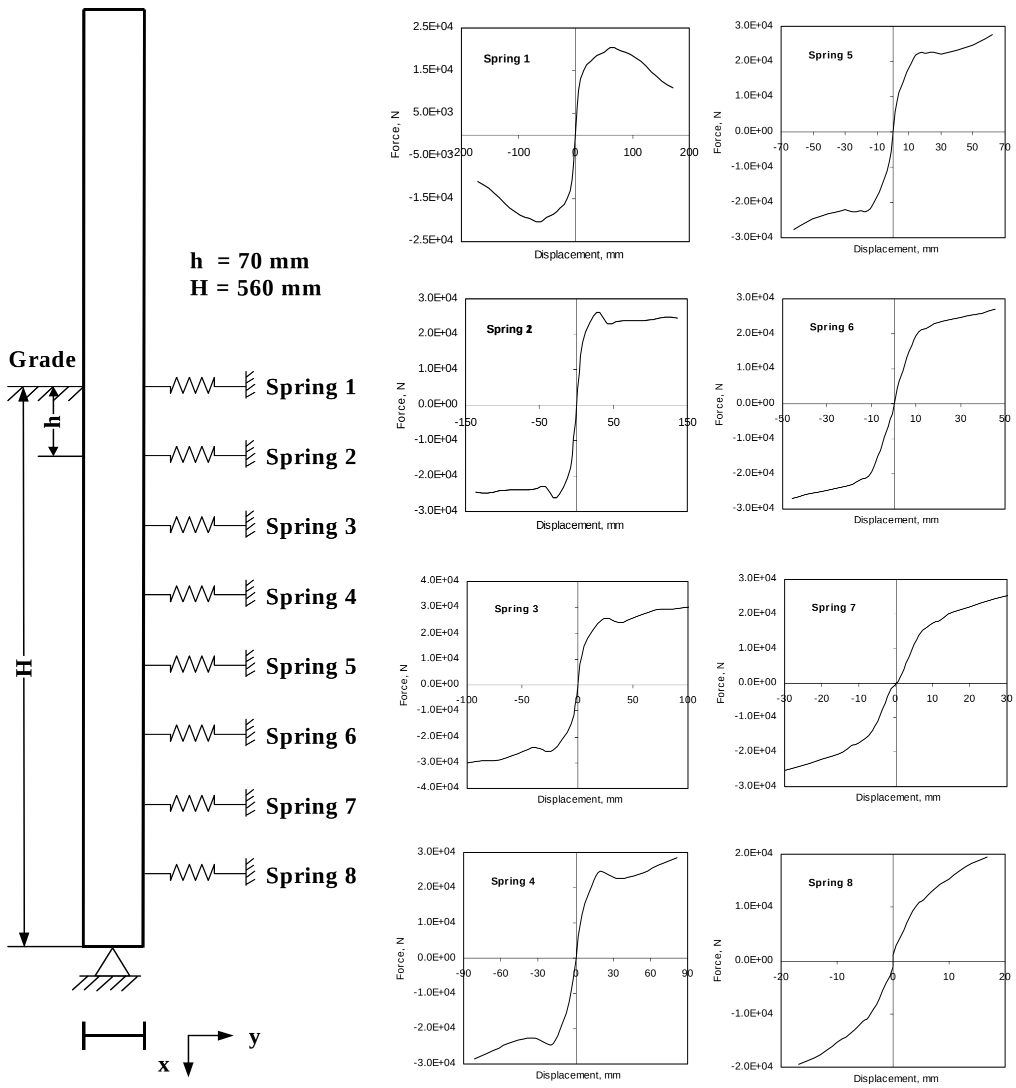

Figure 21. Nonlinear axial springs in the modified FE model (along the post web)

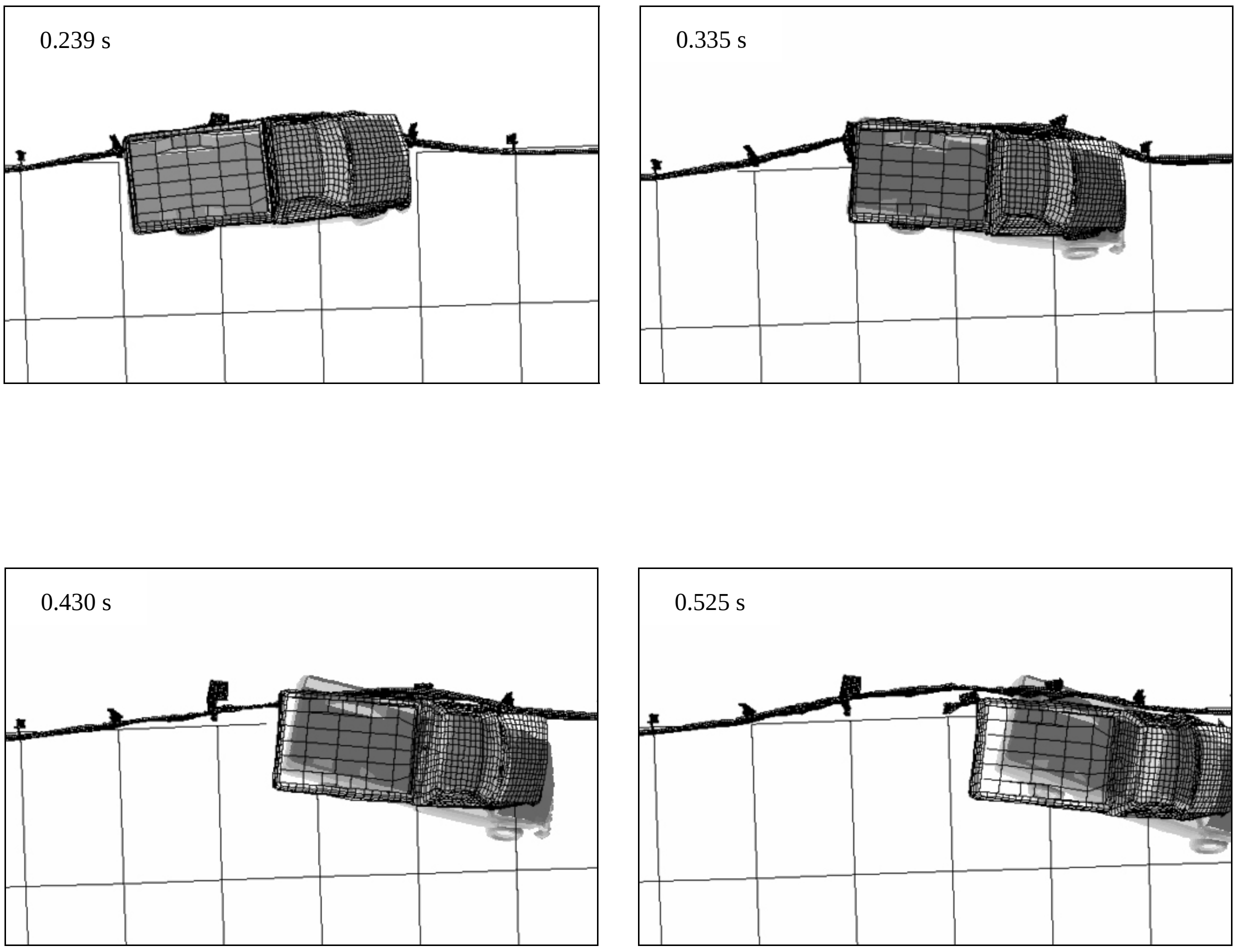

Figure 22. Comparison of sequential overhead views between two FE simulations
Mesh: Modified FE Model (vehicle and guardrail)
Solid: Original FE Model (vehicle only)

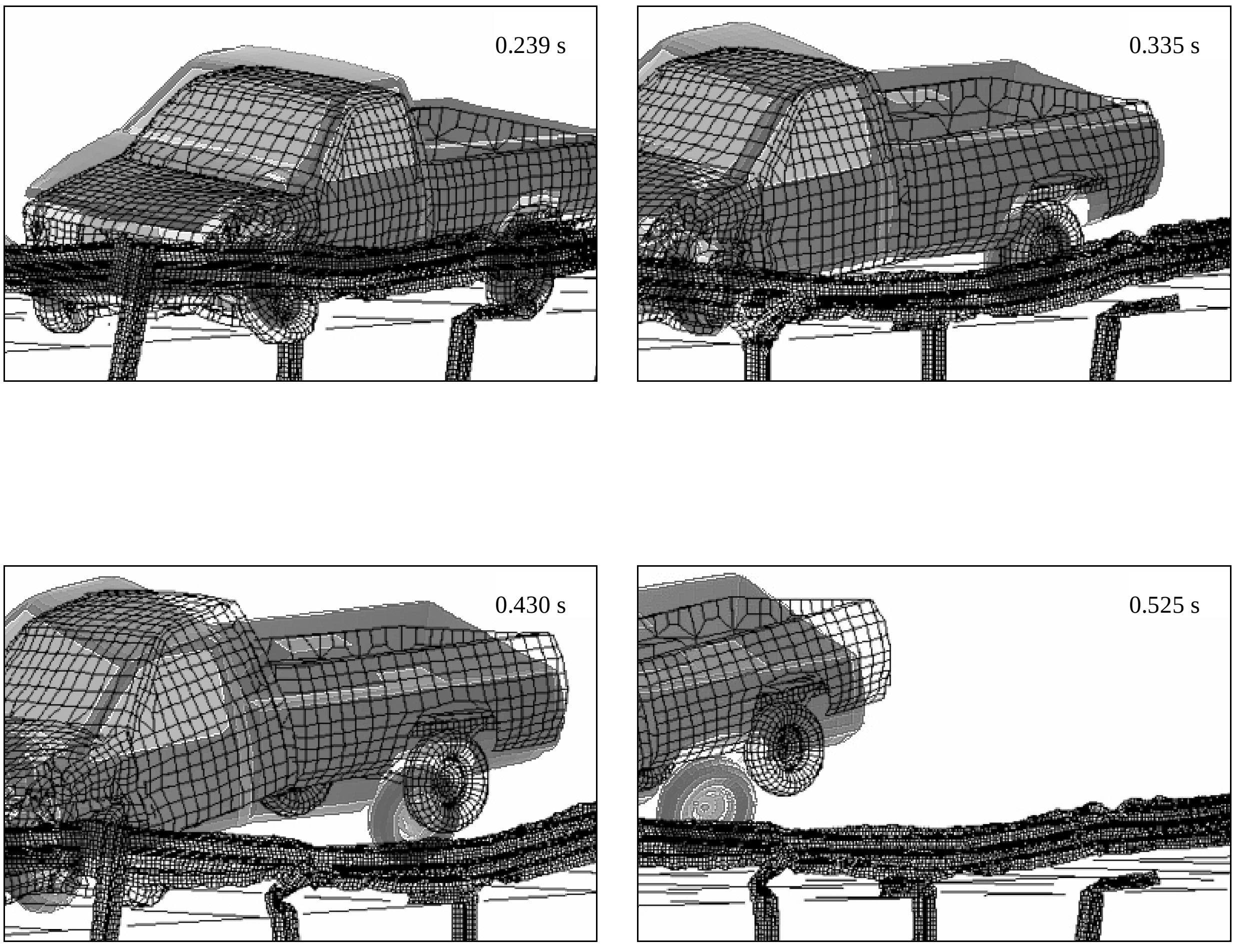

Figure 23. Comparison of sequential frontal views between two FE simulations
Mesh: Modified FE Model (vehicle and guardrail)
Solid: Original FE Model (vehicle only)

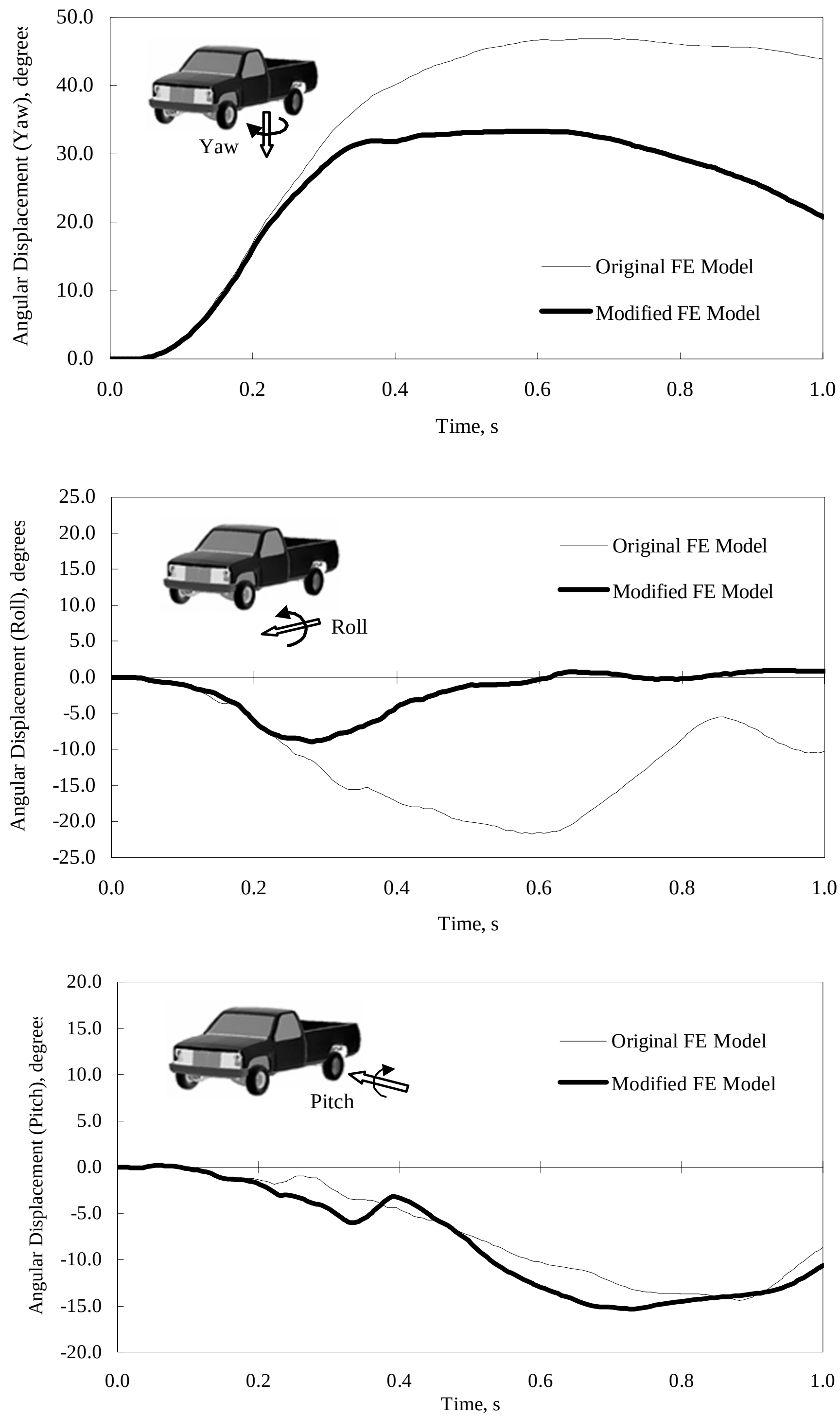

Figure 24. Comparison of vehicle angular displacements (yaw, roll and pitch)

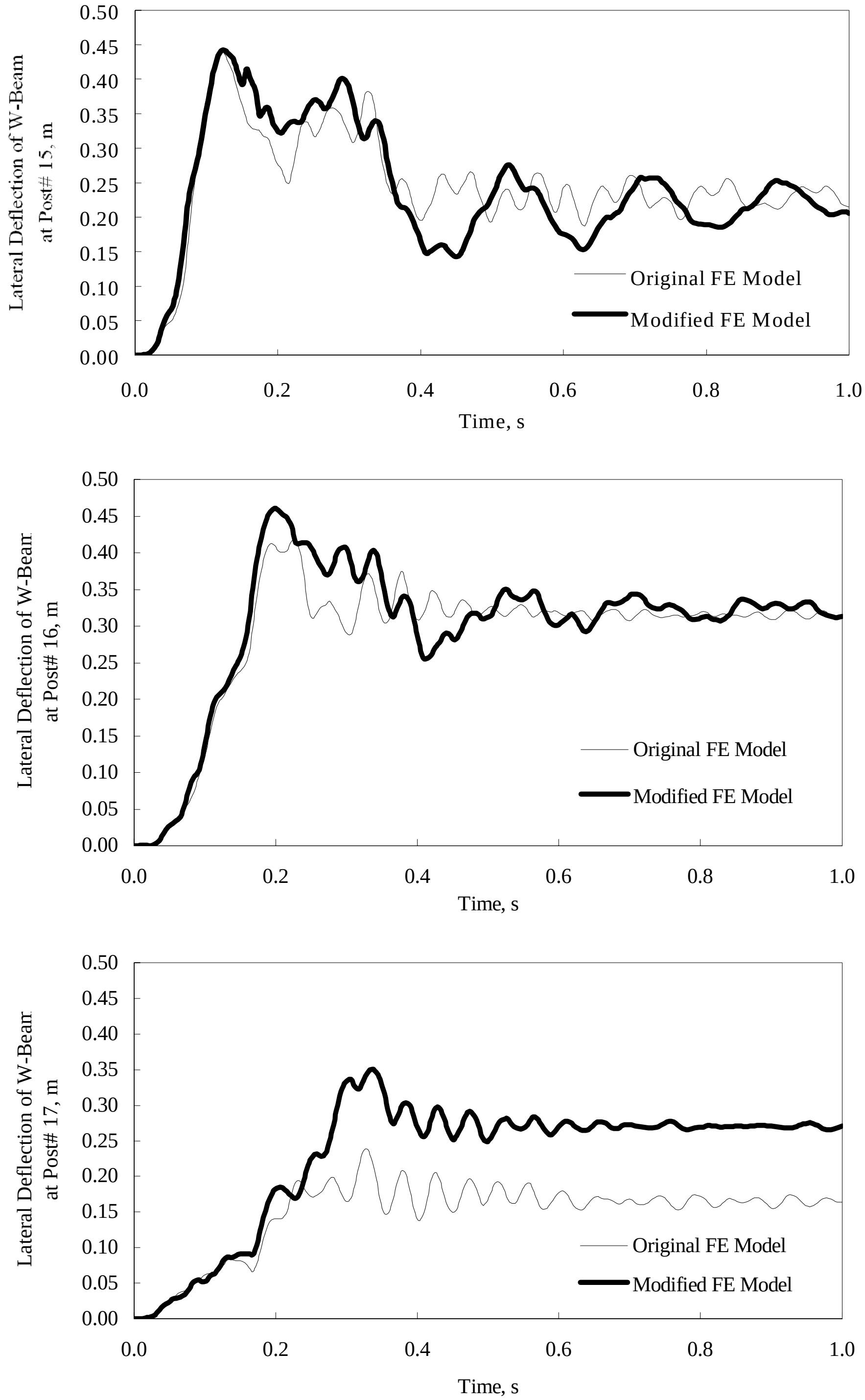

Figure 25. Comparison of the lateral deflection of the W-beam at posts 15, 16 and 17

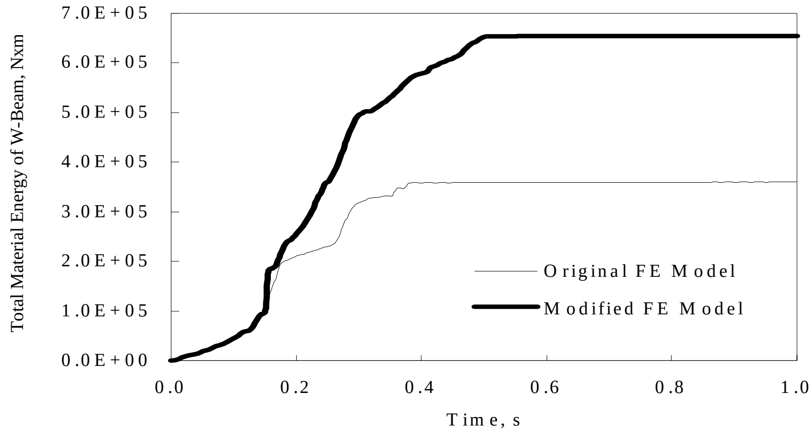

Figure 26. Comparison of the absorbed energy by the W-beam